Supporting Information

Tuning of Surface Oxygen Vacancies for enhancing Photocatalytic Performance under Visible Light Irradiation in Sb_2WO_6 Nanostructures

Manisha Sharma, Rahul Singh, Anitya Sharma and Venkata Krishnan*

School of Chemical Sciences and Advanced Materials Research Center,

Indian Institute of Technology Mandi, Mandi 175075, Himachal Pradesh, India.

Email: vkn@iitmandi.ac.in

Materials characterization

Powder X-ray diffraction (PXRD) measurements were done in 2θ ranging from 5° to 80° by using Rikagu SmartLab rotating anode x-ray diffractometer (9 kV) with Ni-filtered Cu K_α irradiation having wavelength 0.1542 nm with a scanning rate of 2 °C min^{-1} with 45 kV and 100 mA. Raman spectroscopic studies were carried out with high-resolution Horiba LabRAM using a 633 nm laser for excitation. FTIR measurements were done on PerkinElmer Spectrum 2 spectrometer in the range 500 to 4000 cm^{-1} using KBr as reference. Photoluminescence (PL) studies were done on Agilent Technologies Cary Eclipse fluorescence spectrophotometer. The absorbance of as-prepared samples was recorded by using diffuse reflectance spectroscopy (DRS) employing polytetrafluoroethylene (PTFE) polymer as a standard on Perkin Elmer UV-visible-NIR lambda 750 spectrophotometer. The morphological studies were done by scanning electron microscope (FEI Nova Nano SEM-450 instrument), and high-resolution images were taken on transmission electron microscopy (TEM) Technai G 20 (FEI) S-twin microscope operating at 200 kV. Energy dispersive x-ray spectroscopy (EDAX) and elemental mapping were done by using the same SEM instrument. X-ray photoelectron spectroscopy (XPS) studies were performed on the samples using ThermoFisher Scientific NEXSA photoemission spectrometer working at 12 kV anode voltage and 6.50 mA filament current using Al K_α (1486.6 eV) anode as a source. The obtained data was analyzed by using Avantage software. The thermogravimetric analysis (TGA) analysis was done on the NETZSCH STA 449 F1 Jupiter, wherein about 2 mg of sample was heated under nitrogen atmosphere from room temperature to 900 °C at a heating rate of 10 °C min^{-1}. The BEL/CAT2 instrument was used for temperature programmed desorption studies (TPD). The Brunauer-Emmett-Teller (BET) surface area studies were carried out at 77 K on Quantachrome Autosorb-iQ-MP-XR system. The photocatalytic experiments were done in a home-built photoreactor setup consisting of two 45 W CFL lamps emitting visible light, and UV-vis spectra of samples collected at various intervals were recorded on Shimadzu UV-2450 spectrophotometer. Further, the degradation products were detected by using Bruker HD compact high resolution mass spectrometer instrument.

Table S1 Calculated crystallite size and lattice strain of SWO and oxygen-vacancy rich DSWO1, DSWO2 and DSWO3 samples.

Sl. No.	**Sample Name**	**Crystallite Size corresponding to $(20\bar{1})$ plane (nm)**	**Lattice Strain (ε)**	**Lattice Parameters (Å)**
1.	SWO	13.36	0.1657	a = 5.94; b = 4.87; c = 9.12
2.	DSWO1	15.48	0.1396	a = 5.91; b = 4.90; c = 9.13
3.	DSWO2	13.09	0.1687	a = 5.92; b = 4.91; c = 9.11
4.	DSWO3	11.49	0.2286	a = 5.92; b = 4.91; c = 9.14

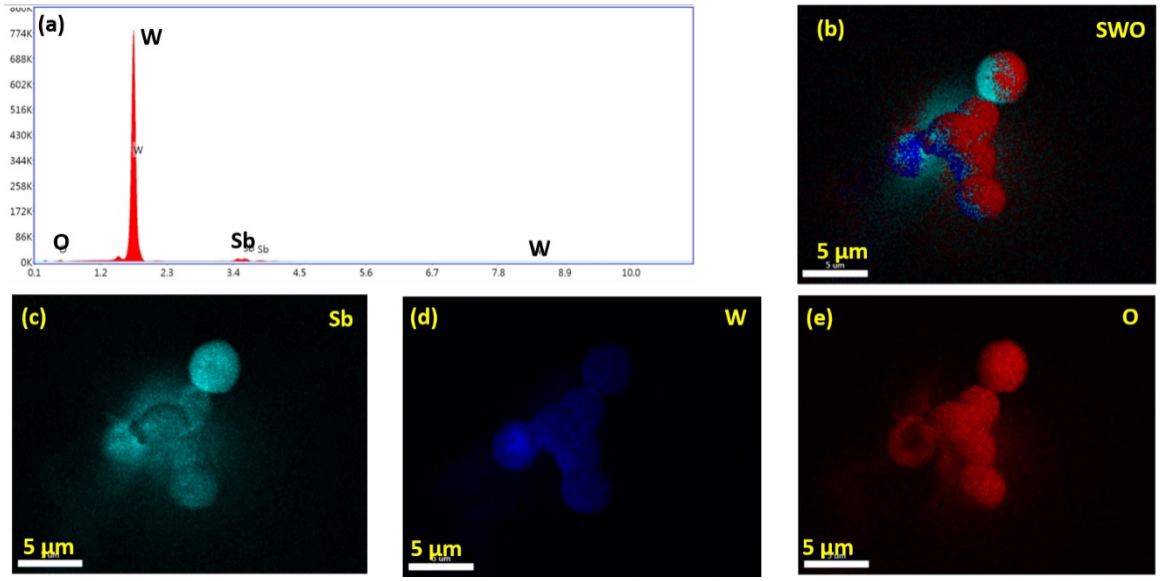

Fig. S1 (a) EDAX spectra and (b-e) elemental spectra of SWO.

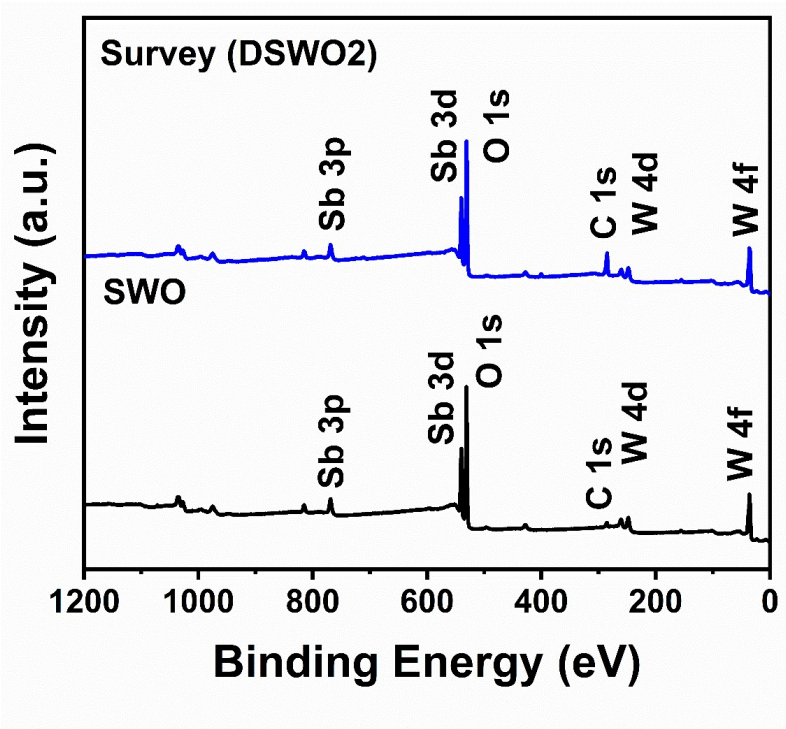

Fig. S2 XPS survey spectra of SWO and DSWO2 samples.

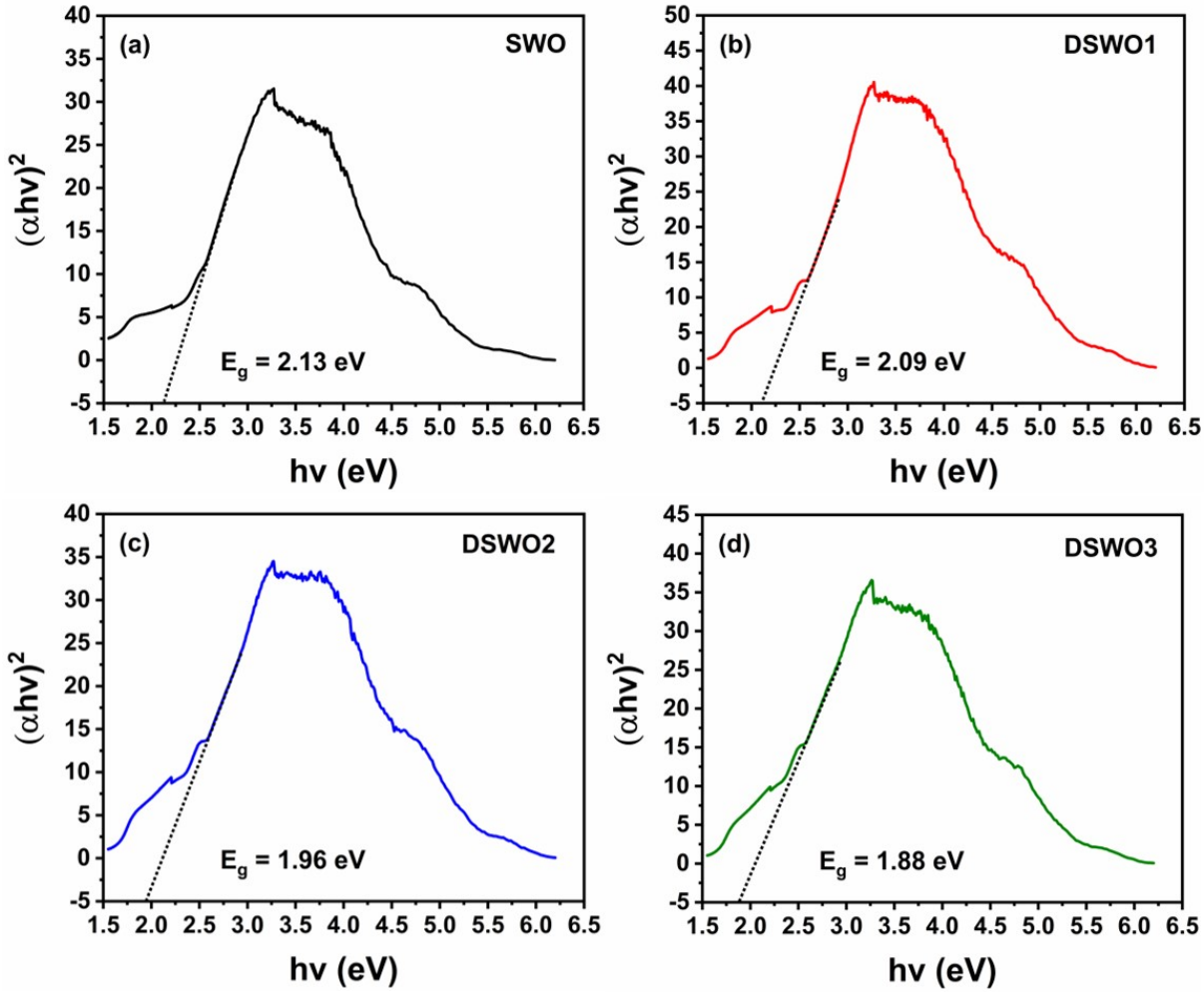

Fig. S3 (a- d) Tauc plots of SWO, DSWO1, DSWO2 and DSWO3 samples.

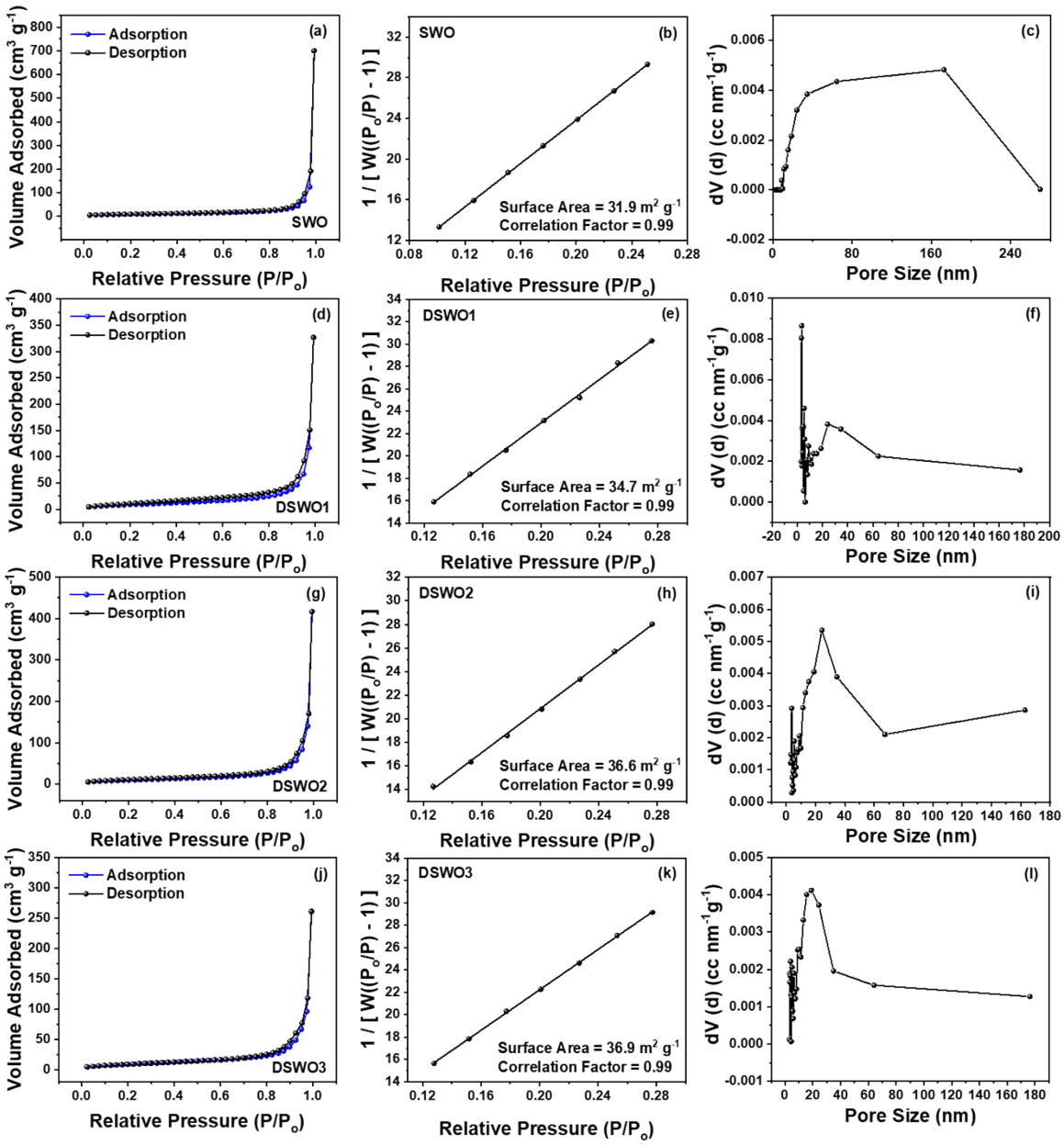

Fig. S4 N_2 adsorption desorption isotherm, multipoint BET and pore size distribution curves for (a, c) SWO, (d, f) DSWO1, (g, i) DSWO2 and (j, l) DSWO3.

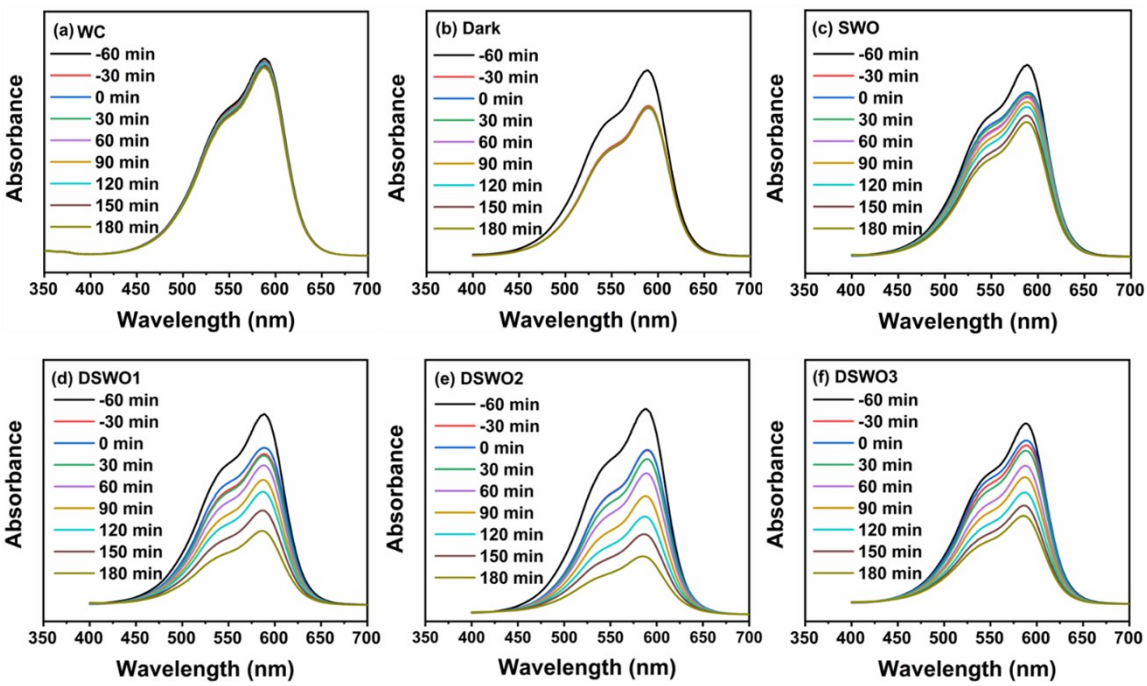

Fig. S5 UV-vis absorption spectra for photocatalytic degradation of CRV dye using (a) WC, (b) dark, (c) SWO, (d) DSWO1, (e) DSWO2 and (f) DSWO3 under visible light irradiation.

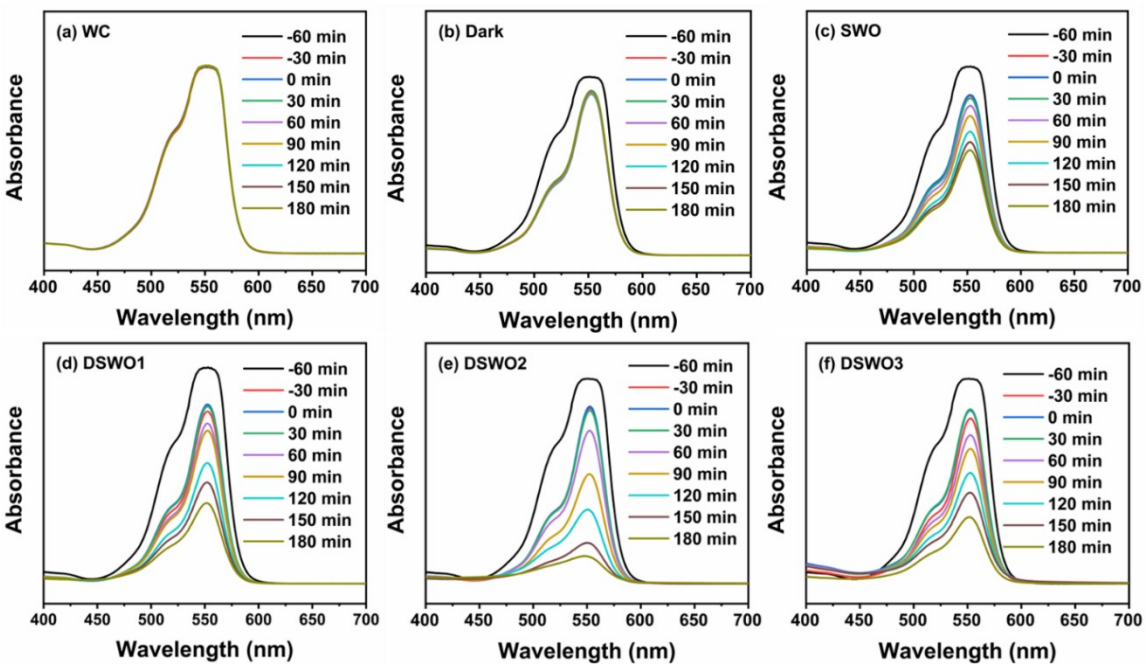

Fig. S6 UV-vis absorption spectra for photocatalytic degradation of RhB dye using (a) WC, (b) dark, (c) SWO, (d) DSWO1, (e) DSWO2 and (f) DSWO3 under visible light irradiation.

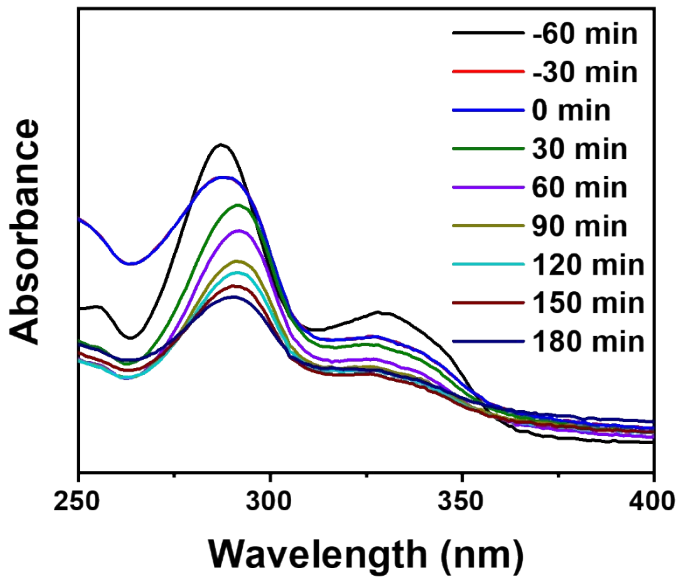

Fig. S7 UV-vis absorption spectra for photocatalytic degradation of LFX over the surface of DSWO2 under visible light irradiation.

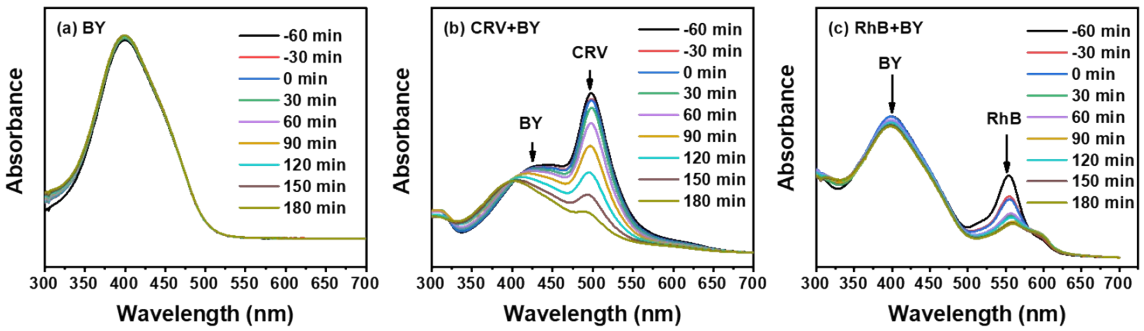

Fig. S8 UV-vis absorption spectra for photocatalytic degradation of (a) BY, (b) CRV+BY and (c) RhB + BY over the surface of DSWO2 under visible light irradiation.

Table S2 Zeta potential values for SWO, DSWO1, DSWO2 and DSWO3.

Sl. No.	Sample Name	Zeta Potential (mV)	Mean Zeta Potential (mV)
1.	SWO	-38.8 -43.0 -42.2	-41.3
2.	DSWO1	-23.9 -22.4 -23.0	-23.1
3.	DSWO2	-19.0 -20.2 -16.8	-18.6
4.	DSWO3	-19.8 -17.2 -17.7	-18.2

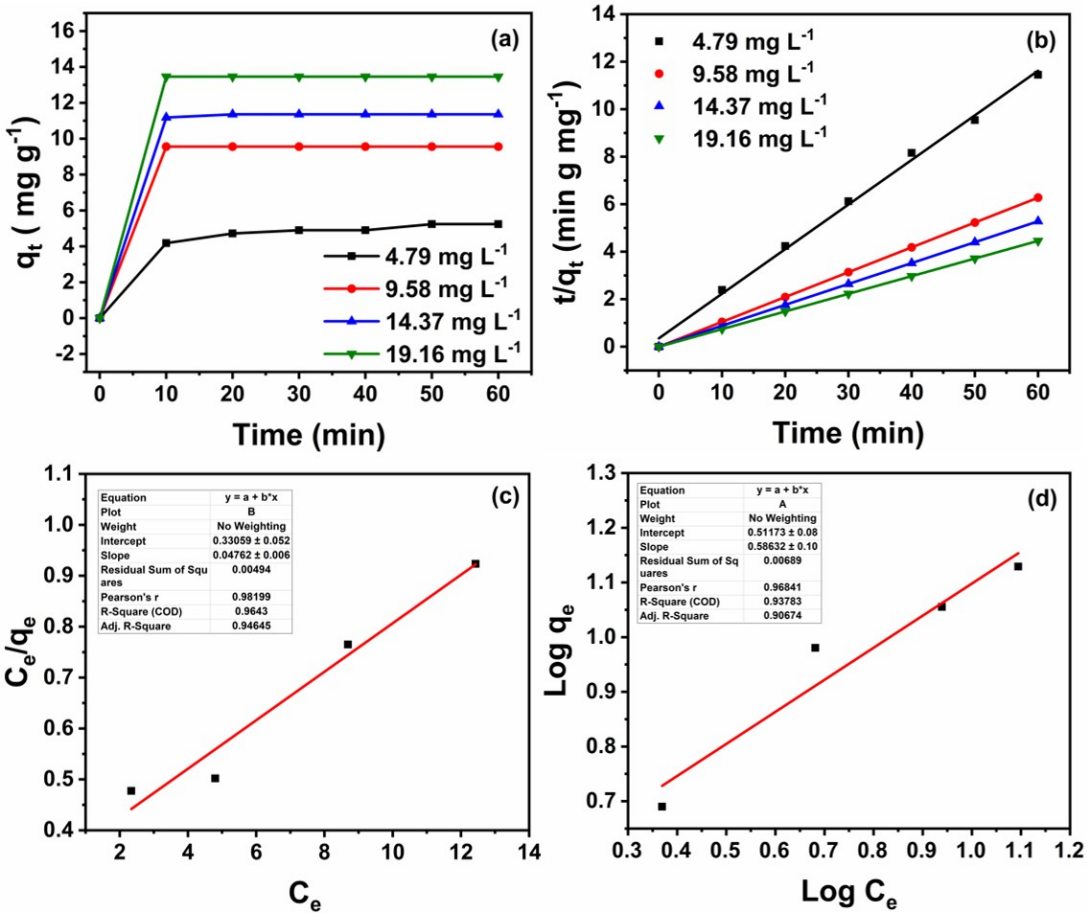

Fig. S9 (a) Time-dependent adsorption study; (b) Pseudo-second-order model for adsorption of RhB on the surface of DSWO2; (c) Langmuir adsorption isotherm and (d) Freundlich adsorption isotherm of RhB on DSWO2.

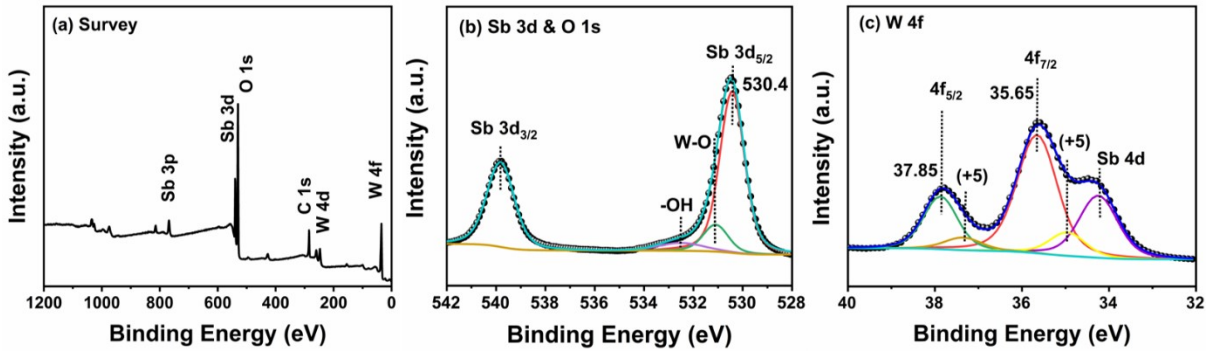

Fig. S10 XPS of recycled DSWO2 photocatalyst.

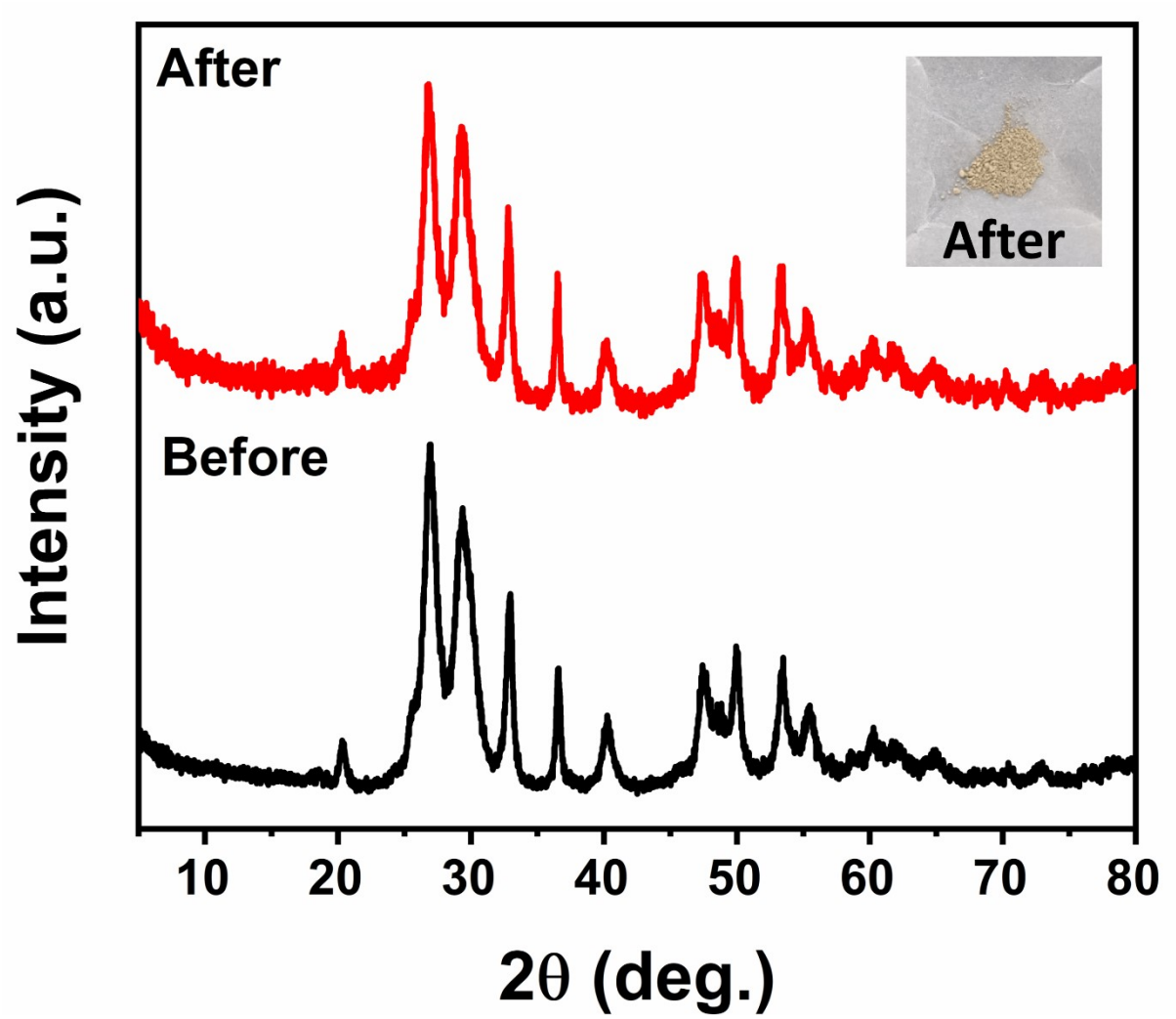

Fig. S11 PXRD of DSWO2 photocatalyst before and after photocatalysis along with the inset of photograph of recycled DSWO2.

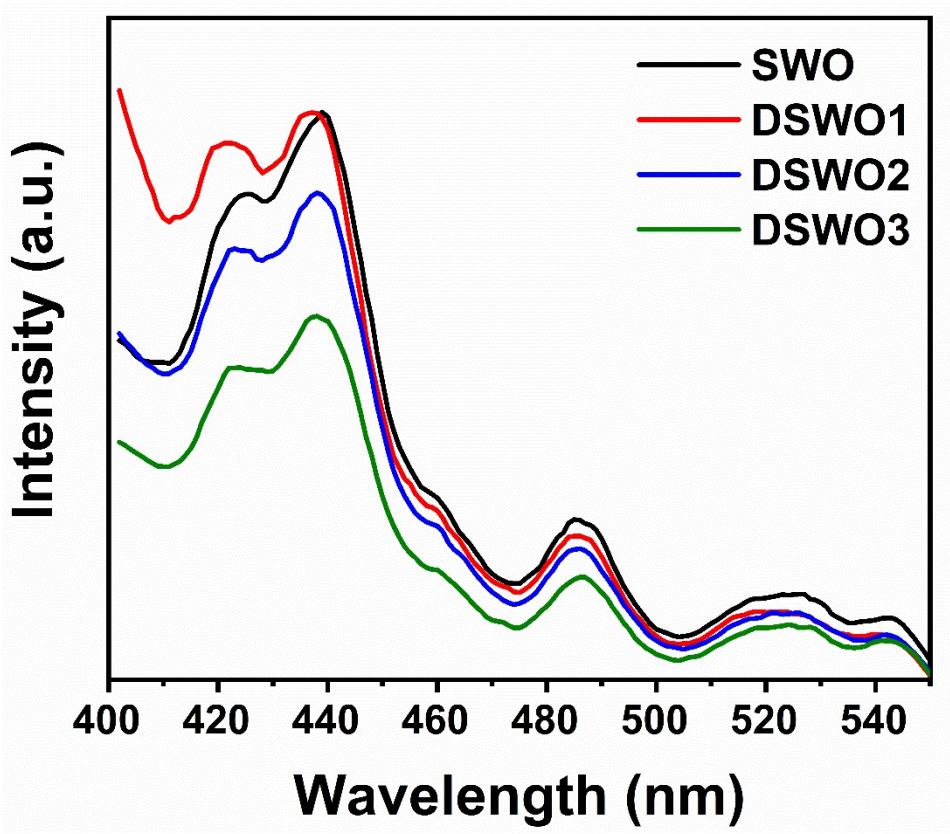

Fig. S12 PL spectra of SWO, DSWO1, DSWO2 and DSWO3 samples.

Table S3 Comparison table of different type of materials towards pollutant degradation.

Sl. No.	Photocatalyst	Pollutant Degraded	Concentration of Pollutant	% Degradation and Time	Rate Constant	Year (Ref.)
1.	La-Mn co-doped Fe_2O_3	Rhodamine B	50 ppm = ≈ (1 X 10^{-4}) M	91.78 % (240 min)	0.0092 min^{-1}	2023[1]
2.	Cd-doped Bi_2MoO_6	Rhodamine B	10 ppm = ≈ (2 X 10^{-5}) M	97.80 % (70 min)	0.0125 min^{-1}	2023[2]
3.	Fe-doped TiO_2	Crystal Violet	10 ppm = ≈ (2.5 X 10^{-5}) M	96 % (180 min)	---------	2023[3]
4.	Tea Leaf Powder/ $ZnIn_2S_4$	Crystal Violet	10 ppm = ≈ (2.5 X 10^{-5}) M	85.36 % (120 min)	---------	2023[4]
5.	Ag_3BiO_3/ZnO/BC	Levofloxacin	10 ppm = ≈ (2.8 X 10^{-5}) M	95.8 % (120 min)	0.0118 min^{-1}	2023[5]
6.	$Sc_2VO_{5-\delta}$/g-C_3N_4	Levofloxacin	12 ppm = ≈ (3.3 X 10^{-5}) M	89.1 % (80 min)	0.0234 min^{-1}	2022[6]
7.	Oxygen vacancy rich Sb_2WO_6	Crystal Violet Rhodamine B Levofloxacin	6 X 10^{-5} M 4 X 10^{-5} M 5 X 10^{-5} M	71 % (180 min) 86 % (180 min) 52 % (180 min)	0.0045 min^{-1} 0.0080 min^{-1} ---	This Work

References

1. S. Maqbool, A. Ahmed, A. Mukhtar, M. Jamshaid, A. U. Rehman and S. Anjum, *Environmental Science and Pollution Research*, 2023, **30**, 7121-7137.
2. B. Zhang, C. Fang, J. Ning, R. Dai, Y. Liu, Q. Wu, F. Zhang, W. Zhang, S. Dou and X. Liu, *Carbon Neutralization*, 2023, **2**, 646-660.
3. A. Mancuso, N. Blangetti, O. Sacco, F. S. Freyria, B. Bonelli, S. Esposito, D. Sannino and V. Vaiano, *Nanomaterials*, 2023, **13**, 270.
4. M. Chand, S. Barthwal, A. S. Rawat, M. Khanuja and S. Rawat, *ACS omega*, 2023, **20**, 17880–17890.
5. G. Dong, W. Chi, D.-f. Chai, Z. Zhang, J. Li, M. Zhao, W. Zhang, J. Lv and S. Chen, *Applied Surface Science*, 2023, **619**, 156732.
6. J. Feng, L. Zu, H. Yang, Y. Zheng, Z. Chen, W. Song, R. Zhao, L. Wang, X. Ran and B. Xiao, *RSC advances*, 2023, **13**, 688-700.